ENO/WENO INTERPOLATION METHODS FOR ZOOMING OF DIGITAL IMAGES

R. M. PIDATELLA, F. STANCO, C. SANTAERA

Dipartimento di Matematica ed Informatica
University of Catania
Viale A. Doria 6 - 95125 Catania, Italy
E-mails: rosa@dmi.unict.it, fstanco@dmi.unict.it, carmelosantaera@tiscali.it

In this paper we address the problem of producing an enlarged picture from a given digital image. We propose a zooming technique based on ENO and WENO schemes that are high order accurate finite difference schemes designed for problems with piecewise smooth solutions containing discontinuities. ENO and WENO schemes have been quite successful in applications, especially for problems containing both shocks and complicated smooth solution structures, such as compressible turbulence simulations and aeroacoustics. The algorithm works both on monochromatic images and RGB color pictures. Our experiments show that the proposed method is better than classical simple zooming techniques (e.g. pixel replication, bilinear interpolation). Moreover our algorithm is competitive both for quality and efficiency with bicubic interpolation.

Keywords: Zooming; Interpolation, ENO, WENO.

1. Introduction

In this paper we address the problem of producing a zoomed picture from a given digital image. This problem arises frequently whenever a user wishes to zoom in to get a better view of a given picture. There are several issues to take into account about zooming: unavoidable smoothing effects, reconstruction of high frequency details without the introduction of artifacts and computational efficiency both in time and in memory requirements. Several good zooming techniques are nowadays well known.[5,7–10,14,19] A generic zooming algorithm takes as input an RGB picture and provides as output a picture of greater size preserving as much as possible the information content of the original image. For a large class of zooming techniques this is achieved by means of some kind of interpolation; replication, bilinear and bicubic are the most popular choices and they are routinely implemented in commercial digital image processing software. Unfortunately, these methods, while preserving the low frequencies content of the source image, are not equally able to enhance high frequencies in order to provide a picture whose visual sharpness matches the quality of the original image. The methods proposed in this paper take into account information about discontinuities or sharp luminance variations while increasing the input picture. The research of new heuristic strategies able to outperform classical image processing techniques is nowadays the key-point to produce digital consumer engine (e.g. Digital Still Camera, 3G Mobile Phone, etc.) with advanced imaging application.[2] The key idea of our algorithm lies at the approximation level, where a nonlinear adaptive procedure is used to automatically choose the locally smoothest stencil, hence avoiding crossing discontinuities in the interpolation procedure as much as possible.

Our experiments show that the proposed method is better, in subjective quality than other well known methods such as pixel replication, bilinear interpolation, LAZA (locally adaptive zooming algorithm).[16] Moreover our algorithm is competitive both for quality and efficiency with bicubic interpolation, b-spline and other traditional techniques of zooming (e.g. Lanczos, s-spline). The technique proposed in this paper is simpler and much faster than fractal based zooming algorithms.[14,17]

The rest of the paper is organized as follows. Section 2 provides a description of ENO and WENO schemes. Section 3 provides a detailed description of the basic algorithm. Section 4 describes how to adapt the proposed algorithm to color images. Section 5 reports the results obtained together with a detailed discussion about related performance and weakness. Section 6 concludes the paper.

2. ENO and WENO schemes

In this section we provide a brief description of ENO and WENO schemes.

2.1. *ENO*

ENO is the first successful attempt to obtain a self similar uniformly high order accurate, yet essentially non-oscillatory, interpolation (i.e. the magnitude of the oscillations decays as $O(\Delta x^k)$ where k is the order of accuracy) for piecewise smooth functions.

In 1D we define cells, cell centers, and cell sizes by:

$$I_i = \left[x_{i-\frac{1}{2}}, x_{i+\frac{1}{2}}\right], \;\; x_i \equiv \frac{1}{2}\left(x_{i-\frac{1}{2}} + x_{i+\frac{1}{2}}\right), \qquad (1)$$
$$\Delta x_i = x_{i-\frac{1}{2}} - x_{i+\frac{1}{2}}, \quad i = 1, 2, \ldots, N$$

We will face the following problem: given the cell averages of a function $v(x)$:

$$\overline{v}_i \equiv \frac{1}{\Delta x_i} \int_{x_{i-\frac{1}{2}}}^{x_{i+\frac{1}{2}}} v(\xi) d\xi \qquad (2)$$

find a polynomial of degree at most $k-1$, for each cell I_i, such that it is a $k-th$ order accurate approximation to the function $v(x)$ inside I_i:

$$p_i(x) = v(x) + O(\Delta x^k), \;\; x \in I_i, \;\; i = 1, \ldots, N \qquad (3)$$

In a given cell I_i, we choose a stencil $S(i)$ based on r cells to the left, s cells to the right, and I_i itself. If the order of accuracy has to be k, we have:

$$S(i) \equiv \{I_{i-r}, \ldots, I_{i+s}\} \qquad (4)$$

There is a unique polynomial $p(x)$ of $k-1$ degree whose cell average in $S(i)$ is that of $v(x)$:

$$\frac{1}{\Delta x_j} \int_{x_{j-\frac{1}{2}}}^{x_{j+\frac{1}{2}}} p(\xi) d\xi = \overline{v}_j \qquad (5)$$

Given the k cell averages $\overline{v}_{i-r}, \ldots, \overline{v}_{i-r+k-1}$ that are constants $c_{r,j}$ such that one can find a reconstructed value at the cell boundary $x_{i+\frac{1}{1}}$:

$$v_{i+\frac{1}{2}} = \sum_{j=0}^{k-1} c_{r,j} \overline{v}_{i-r+j} \qquad (6)$$

which is k-order accurate.[1]

To determine the local stencil, we develop a hierarchy that begins with one cell

$$S(i) = I_i = \left\{x_{i-\frac{1}{2}}, x_{i+\frac{1}{2}}\right\} \qquad (7)$$

and adds one cell at a time to the stencil from the two candidates on the left and on the right, based on the size of the two relevant Newton divided differences

$$v\left[x_{i-\frac{3}{2}}, x_{i-\frac{1}{2}}, x_{i+\frac{1}{2}}\right] \quad \text{and} \quad v\left[x_{i-\frac{1}{2}}, x_{i+\frac{1}{2}}, x_{i+\frac{3}{2}}\right] \qquad (8)$$

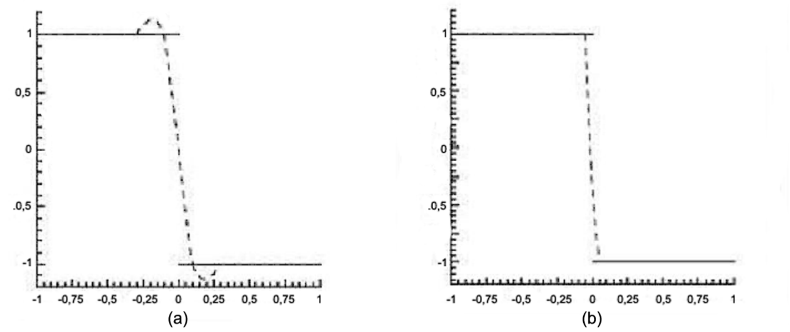

Fig. 1. (a) Fixed central stencil cubic interpolation; (b) ENO cubic interpolation for the step function. Solid: exact function; Dashed: interpolant piecewise cubic polynomials.

We choose the one with the least absolute value, achieving:

$$S(i) = \{I_{i-1}, I_i\} \equiv \left\{x_{i-\frac{3}{2}}, x_{i-\frac{1}{2}}, x_{i+\frac{1}{2}}\right\} \tag{9}$$

$$S(i) = \{I_i, I_{i+1}\} \equiv \left\{x_{i-\frac{1}{2}}, x_{i+\frac{1}{2}}, x_{i+\frac{3}{2}}\right\} \tag{10}$$

This procedure goes forward until we obtain the number of required points in the stencil.

Once we have defined the stencil

$$S(i) = \{I_{i-r}, \ldots, I_{i+s}\}, \quad k = r + s + 1 \tag{11}$$

one can compute the Eq. 6 where the constants $c_{r,j}$ depend on r, k and Δx^k.

We can find the constants $c_{r,j}$ from the Lagrange polynomials and the non-oscillatory behavior is provided by adapting the stencil. Fig. 1 shows the differences differences between the cubic interpolation and the ENO cubic interpolation.

2.2. *WENO*

Differently to ENO, in WENO schemes one uses a convex combination of all the stencils. Suppose the k candidate stencils

$$S_r(i) = \{x_{i-r}, \ldots, x_{i-r+k-1}\}, \quad r = 0, \ldots, k-1 \tag{12}$$

produce k different reconstructions to the value $v_{i+\frac{1}{2}}$:

$$v^{(r)}_{i+\frac{1}{2}} = \sum_{j=0}^{k-1} c_{r,j}\overline{v}_{i-r+j}. \tag{13}$$

Then we combine polynomials using weights ω_r

$$v_{i+\frac{1}{2}} = \sum_{r=0}^{k-1} \omega_r v^{(r)}_{i+\frac{1}{2}} \tag{14}$$

with $\sum_{r=0}^{k-1} \omega_r = 1$.

The weights ω_r are calculated using the following equations:

$$\omega_r = \frac{\alpha_r}{\sum_{s=0}^{k-1}\alpha_s}, \;\; \alpha_r = \frac{d_r}{\beta_r}, \;\; \beta_r = \sum_{l=1}^{k-1} \Delta x^{2l-1} \int_{x_{i-\frac{1}{2}}}^{x_{i+\frac{1}{2}}} \left(\frac{\partial^l p_r(x)}{\partial x^l}\right) dx \tag{15}$$

where β_r are the "*smoothness indicators*" and d_r is always positive and it satisfies the condition

$$\sum_{r=0}^{k-1} d_r = 1 \tag{16}$$

Many versions of WENO schemes have been developed in the last few years. These methods differ from WENO schemes in the dimension of the stencil or in the calculation of the "smoothness indicators". Some of these schemes are: OWENO (Optimized-WENO);[3] CWENO (Central-WENO);[4] WENO5M (Fifth-Order Mapped WENO).[6]

3. The proposed algorithm

In this section, we give a detailed description of the proposed algorithm. If S is a gray level image whose size is $n \times n$, the zooming algorithm creates a new image Z of size $(2n-1) \times (2n-1)$. Initially, the image Z contains pixels with known values and pixels unknown. More precisely, as first step the algorithm expands the source image S into a regular grid Z. Fig. 2(a) shows schematically the mapping function $E : S \rightarrow Z$ that disposes the original pixels into the new image. The expansion follows the equation:

$$E(S(i,j)) = Z(2i-1, 2j-1), \;\; i,j = 1,2,\ldots,n. \tag{17}$$

The mapping E leaves undefined the value of all the pixels in Z with at least one even coordinate (white dots in Fig. 2(a)).

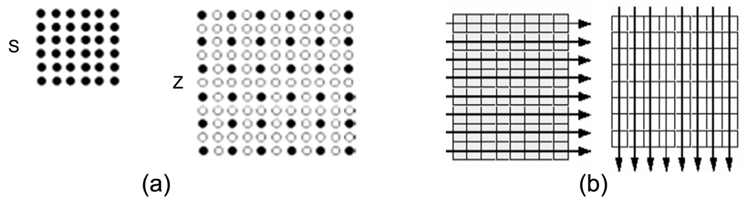

Fig. 2. (a) Zooming enlargement; (b) Scan order.

The second step of the algorithm is different if the approach is ENO or WENO based. It always works over the pixels still undefined. More precisely, first we interpolate the pixels in the odd rows and then all the others (Fig. 2(b)).

In the ENO Approach, if k is the degree of the method, the cell $I_{i,j}$ starts with a two point stencil

$$S_2(i,j) = \{x_{i,j-1}, x_{i,j+1}\} \tag{18}$$

For $l = 2, \ldots, k$ assuming

$$S_l(i,j) = \{x_{i,j+1}, \ldots, x_{i,j+2l-1}\} \tag{19}$$

is known, add one of the two neighboring points $x_{i,j-1}$ or $x_{i,j+2l+1}$ to the stencil, following the ENO procedure specified in section 2.1.

Once the stencil is found, we can calculate $v_{i,j}$ following the:

$$v_{i,j} = \sum_{l=0}^{k-1} c_{r,l} v_{i,j-(2r+1)+2l} \tag{20}$$

with r is the number of stencils at the left of I_i, and the coefficient $c_{r,l}$ are defined in.[1]

In the WENO approach, if the k candidate stencils are computed using ENO procedure in Eq. 19:

$$S_r(i,j) = \{x_{i,j-2r-1}, \ldots, x_{i,j-2r+2k-1}\}, \;\; r = 0, \ldots, k-1 \tag{21}$$

we produce k different reconstructions to the value $v_{i,j}$

$$v_{i,j}^{(r)} = \sum_{l=0}^{k-1} c_{r,l} v_{i,j-(2r+1)+2l}, \;\; r = 0, \ldots, k-1 \tag{22}$$

The constants d_r, and the *smoothness indicators* β_r, for all $r = 0, \ldots, k-1$ are described in Section 2.2.

The final reconstruction is

$$v_{i,j} = \sum_{r=0}^{k-1} \omega_r v_{i,j}^{(r)} \tag{23}$$

4. Zooming color pictures

The basic algorithm described above for gray scale pictures can be easily generalized to the case of RGB colored digital images. To change the space color we take advantage of the higher sensitivity of human visual system to luminance variations with respect to chrominance values. Hence it makes sense to allocate larger computational resources to zoom luminance values, while chrominance values may be processed with a simpler and more economical approach. This simple strategy is inspired by analogues techniques used by classical lossy image compression algorithms like JPEG and/or JPEG2000 vastly implemented in almost digital still camera engines.
Accordingly we propose to operate as follows:

- Translate the original RGB picture into the YUV color model.
- Zoom the luminance values Y according with the basic algorithm described above.
- Zoom the U and V values using a simpler pixel replication algorithm.
- Back translates the zoomed YUV picture into an RGB image.

The results obtained with this basic approach are qualitatively comparable with the results obtained using bicubic interpolation over the three color channels. From the computational point of view, it is important to note how no significant difference in terms of timing response has been observed between the simple application of our approach to the three RGB planes and the approach described above (RGB-YUV conversion, Y zooming U, V replication, YUV-RGB conversion). Yet, in real applications (DSC, 3G Mobile phone,) the zooming process inside typical Image Generation Pipeline if present is realized just before compression: the YUV conversion is always performed as a crucial step to achieve visual lossless compression. In this case the color conversion itself does not introduce further computational costs.

5. Experimental results

The validation of a zooming algorithm requires the assessment of the visual quality of the zoomed pictures. Fig. 3 shows three examples of zooming pictures obtained with the proposed algorithm. Unfortunately this qualitative judgment involves qualitative evaluation of many zoomed pictures from a large pool of human observers and it is hard to be done in a subjective and precise way. For this reason several alternative quantitative measurements related to picture quality have been proposed and widely used in the literature. To validate our algorithm we have chosen both the approaches proposed in Refs.,[11,12,15] classical metrics and subjective tests. In particular we have used the cross-correlation and the PSNR (Peak Signal Noise to Ratio) between the original picture and the reconstructed picture to assess the quality of reconstruction. In our experimental contest we have first collected a test pool of 100 gray scale pictures. For each image I in this set we have first performed the following operations:

- reduction by decimation: a new picture I_d of half size of I is obtained taking only the pixels with both odd coordinates of the original picture;
- starting from I_d we have obtained the zoomed image;
- calculation of the following quantitative measurements between the original picture and the reconstructed picture: PSNR, cross-correlation coefficient and error threshold;
- calculation of the cpu-time;
- qualitative evaluation of the zoomed image.

The cross-correlation coefficient C between two pictures A and B is:

$$C = \left| \frac{\left(\sum_{k,l} A(k,l)B(k,l) - KLab\right)}{\sqrt{\left(\sum_{k,l} A^2(k,l) - KLa^2\right)\left(\sum_{k,l} B^2(k,l) - KLb^2\right)}} \right| \tag{24}$$

where a and b denote, respectively, the average value of picture A and B, K and L denote, respectively, width and length, in pixels, of images A and B. Notice that cross-correlation coefficients is between 0 and 1. The more the coefficient approaches 1, the better the reconstruction quality. The PSNR is calculated using the classical equation.

We have chosen simple replication, LAZA algorithm, bilinear and bicubic interpolation as comparing stones to assess the quality of our technique. It is generally accepted that replication provides the worst quality-wise zooming algorithm while bicubic interpolation is considered one of the best options available. Table 1 and Table 2 show experimental results related, respectively, to ENO and WENO based algorithms of zooming.

Fig. 3. (a) Original images; Examples of zoomed pictures with the Bryson-Levy (b) and Russo-Ferretti (c) based methods.

Table 1. ENO results

	CPU Time	Cross-Correlation	PSNR
ENO2	5,23	0,9858	29,42
ENO3	15,72	0,9847	29,06
ENO4	34,38	0,9826	28,44
ENO5	71,58	0,9852	23,35
ENO3-Cross	15,18	0,9898	30,83
LAZA	12,75	0,9946	33,58
Replication	0,07	0,9854	29,32
Spline	0,93	0,9952	34,27
Bilinear	0,43	0,995	33,95
Bicubic	1,05	0,9953	34,36

The numerical results illustrated in these tables says that ENO schemes achieve not too good results if applied to the zooming $\times 2$ of a digital image due to the higher cpu-time, the quantitative measurements worse than bicubic and LAZA, and do not give good quality images. However, the WENO schemes achieve very good results with small cpu-time, with quantitative measurements comparable to bicubic, and give good quality images.

The graphs in Fig. 4 show the average percentage of errors observed over the test pool as different tolerance threshold are considered. The WENO

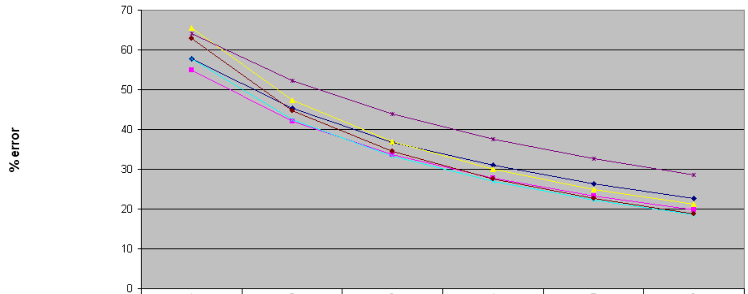

	1	2	3	4	5	6
WENO 3	57,84	45,34	36,78	30,97	26,33	22,69
WENO 5	54,93	42,09	33,76	27,85	23,30	19,80
WENO 7	65,45	47,37	36,99	30,04	24,90	21,31
LAZA	57,72	42,38	33,28	26,88	22,15	18,54
REPLCATION	64,03	52,29	43,95	37,65	32,61	28,54
BICUBIC	62,87	44,68	34,48	27,61	22,67	18,83

Threshold error

(a)

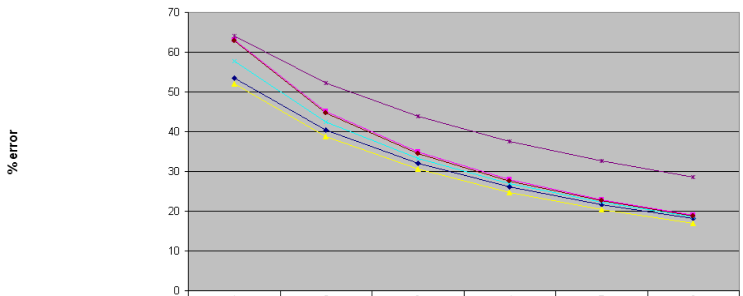

	1	2	3	4	5	6
RUSSO-FERRETTI 2-3	53,5	40,34	32,03	26,04	21,57	18,07
RUSSO-FERRETTI 3-5	63,02	45,14	34,81	27,92	22,83	19,05
BRYSON LEVY	52,1	38,77	30,52	24,68	20,37	17,04
LAZA	57,72	42,38	33,28	26,88	22,15	18,54
REPLICATION	64,03	52,29	43,95	37,65	32,61	28,54
BICUBIC	62,87	44,68	34,48	27,61	22,67	18,83

Threshold error

(b)

Fig. 4. Error values with different thresholds

Russo-Ferretti[13] and Bryson-Levy[18] methods are always the best, since their values are always lower than the others.

6. Conclusions

In this paper we have proposed a new technique for zooming a digital picture, both in gray scale and in RGB colors. The experimental results show that satisfying results are obtained using the Russo-Ferretti and Bryson-

Table 2. WENO results

	CPU Time	Cross-Correlation	PSNR
WENO3	1,08	0,9902	30,94
WENO5	1,5	0,9924	32,11
WENO7	1,86	0,9936	32,73
WENO7-2D	2,1	0,9946	33,47
OWENO1-2D	2,14	0,9947	33,58
Russo-Ferretti 2-3	1,56	0,9953	34,06
Russo-Ferretti 3-5	1,95	0,9957	34,34
Bryson Levy	1,46	0,9956	34,33
LAZA	12,99	0,995	33,58
Replication	0,05	0,9871	29,32
Spline	0,75	0,9955	34,27
Bilinear	0,42	0,9953	33,95
Bicubic	1,01	0,9957	34,36

Levy versions of WENO schemes. These proposed methods beat in quality pixel replication, bilinear and bicubic interpolation, LAZA algortihm. Moreover, the proposed algorithms are competitive both for quality and efficiency with other traditional techniques of zooming. Moreover, these algorithms preserve the image edges (major transition light-shade zones) in any direction without the introduction of artifacts and without to put out of focus the resulting images. The tests prove that these methods are very good to zooming medical pictures and images including writings. The proposed method, while of not greater complexity than bicubic interpolation provides qualitatively better results.

References

1. C.-W. Shu, Essentially Non-Oscillatory and Weighted Essentially Non-Oscillatory Schemes for Hyperbolic Conservation Laws, in Advanced numerical approximation of nonlinear hyperbolic equations, LNM1697, Ed. A. Quarteroni, pp.325-432, Spinger, 1997.
2. S. Battiato, M. Mancuso, An introduction to the digital still camera technology, ST Journal of System Research, Special Issue on Image Processing for Digital Still Camera, vol. 2, issue 2, 2001.
3. Z. J. Wang and R. F. Chen, Optimized Weighted Essentially Nonoscillatory Schemes for Linear Waves with Discontinuity, Journal of Computational Physics 174, pp. 381-404, 2001.
4. D. Levy, G. Puppo and G. Russo, Central WENO Schemes for Hyperbolic Systems of Conservation Laws, M2AN, Vol. 33, No 3, pp. 547-571, 1999.
5. D.F. Florencio, R.W. Schafer, Post-sampling aliasing control for images, Proceedings of International Conference on Acoustics, Speech and Signal Processing, Detroit, MI 2, pp. 893-896, 1995.

6. A. K. Henrick, T. D. Aslam, J. M. Powers, Mapped weighted essentially non-oscillatory schemes: Achieving optimal order near critical points, Journal of Computational Physics, vol. 207, issue 2, pp. 542-567, 2005.
7. H.S. Hou, H.C. Andrews, Cubic splines for image interpolation and digital filtering, IEEE Transactions on Acoustics, Speech, Signal Processing ASSP-26, issue 6, pp. 508-517, 1978.
8. A.K. Jain, Fundamentals of Digital Image Processing, Prenctice-Hall, Englewood Cliffs, NJ, 1989.
9. R.G. Keys, Cubic convolution interpolation for digital image processing, IEEE Transactions. on Acoustics, Speech, Signal Processing vol. 29, issue 6, pp. 1153-1160, 1981.
10. S.W. Lee, J.K. Paik, Image interpolation using adaptive fast B-spline filtering, Proceedings of International Conference on Acoustics, Speech, and Signal Processing vol. 5, pp. 177-179, 1993.
11. T.M. Lehmann, C. Gonner, K. Spitzer, Survey: interpolation methods in medical image processing, IEEE Transactions on Medical Imaging vol. 18, issue 11, 1999.
12. E. Maeland, On the comparison of interpolation methods, IEEE Transactions on Medical Imaging MI-7, pp. 213-217, 1988.
13. E. Carlini, R. Ferretti, G. Russo, A Weighted Essentially Non-oscillatory, large time-step schemes for Hamilton-Jacobi Equations, SIAM J. Sci. Comp., vol 27, pp. 1071-1901, 2005.
14. D.M. Monro, P.D. Wakefield, Zooming with implicit fractals, Proceedings of International Conference on Image Processing ICIP97 vol. 1, pp. 913-916, 1997.
15. J.A. Parker, R.V. Kenyon, D.E. Troxel, Comparison of interpolating methods for image resampling, IEEE Transactions on Medical Imaging MI-2, pp. 31-39, 1983.
16. S. Battiato, G. Gallo, F. Stanco, A locally adaptive zooming algorithm for digital images, Elsevier Image and. Vision Computing, vol. 20, issue 11, 2002.
17. E. Polidori, J.L. Dugelay, Zooming using iterated function systems, NATO ASI Conference on Fractal Image Encoding and Analysis, Trondheim, Norway,1995.
18. Steve Bryson, Doron Levy, High-Order Central Weno Schemes for multidimensional Hamilton-Jacobi equations, SIAM Journal on Numerical Analysis, vol. 41, pp.1339-1369, 2003.
19. P.V. Sankar, L.A. Ferrari, Simple algorithms and architecture for Bspline interpolation, IEEE Transactions on Pattern Analysis Machine Intelligence PAMI vol. 10, pp. 271-276, 1988.